# Nanofiber-shaped $Co_3O_4$@$In_2O_3$ composite for high-performance enzymeless glucose sensing

Xinda Xu [a], Chao Zhang [a], Woochul Yang [b*], Yujia Li [c], Bing Li [c*], Yuvaraj Haldorai [d], Jiang Zhenyu [e], Wanfeng Xie [a,c*]

a. College of Electronics & Information, Qingdao University, Qingdao 266071, China.

b. Department of Physics, Dongguk University, Seoul 04620, South Korea.

c. Institute for Materials Discovery, Department of Chemistry, University College London, London, WC1E 7JE UK.

d. Department of Chemistry (SF), PSG College of Arts and Science, Coimbatore, 641014, Tamilnadu,India

e. School of Integrated Circuits, Shandong University, Jinan 250100, PR China

* To whom correspondence should be addressed

Wanfeng Xie: wfxie@qdu.edu.cn

Bing Li: bing.li@ucl.ac.uk

Details of the instruments required for material characterisation and electrochemical property testing：

The microscopic structure of the samples was analyzed and characterized through X-ray diffraction (XRD) technique, employing a Bruker D8 diffractometer that utilized Cu Kα radiation (λ = 0.154 nm). The elemental makeup of the samples was investigated through X-ray photoelectron spectroscopy (XPS), utilizing a Termo Scientific Escalab 250xi instrument that was fitted with a monochromatic Al Kα radiation source. The surface morphology of the nanofibers was visualized using a field emission scanning electron microscope (FESEM, Zeiss Gemini 500). The samples were structurally characterized using a FEI Tecnai G2 F20 transmission electron microscope (TEM). TEM analyses included low magnification plain TEM images and scanning transmission electron microscopy (STEM). The JEM-2100 (Jeol, Japan) high-resolution transmission electron microscope (HRTEM) was employed to scrutinize the particle dimensions and structural characteristics of the resultant $Co_3O_4$@$In_2O_3$ NFs system. All electrochemical assessments, encompassing cyclic voltammetry (CV) experiments and current-time (I-t) measurements, were conducted utilizing a CHI 760E electrochemical workstation from CH Instruments, Inc., USA, within a standard three-electrode configuration. ITO or $Co_3O_4$ NFs/ITO or $Co_3O_4$@$In_2O_3$ NFs/ITO, platinum sheet and Ag/AgCl/KCl electrodes were used as the working, counter and reference electrodes, respectively.

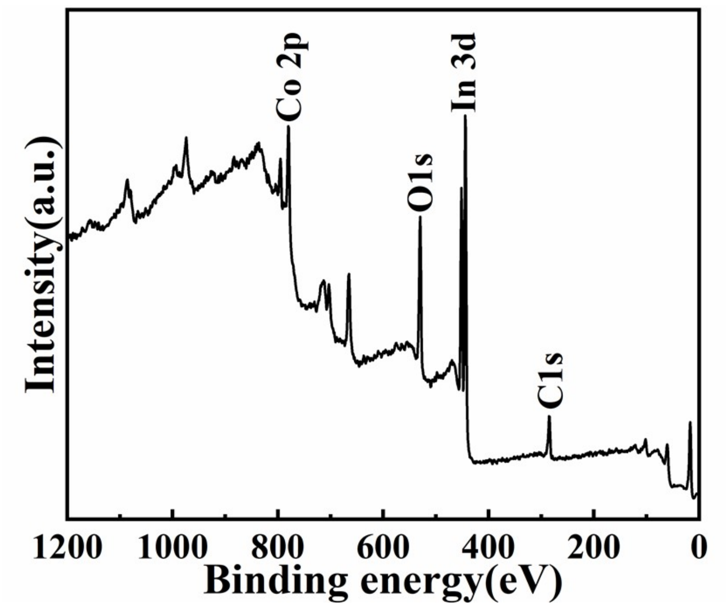


Figure S1. XPS spectra of $Co_3O_4$ NFs/$In_2O_3$.

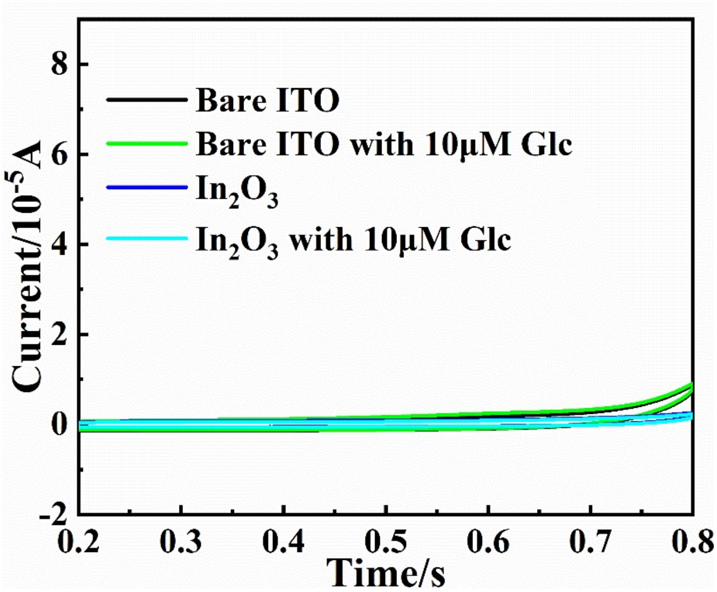


Figure S2 CV curves of bare ITO electrode and $In_2O_3$ electrode with and without glucose.

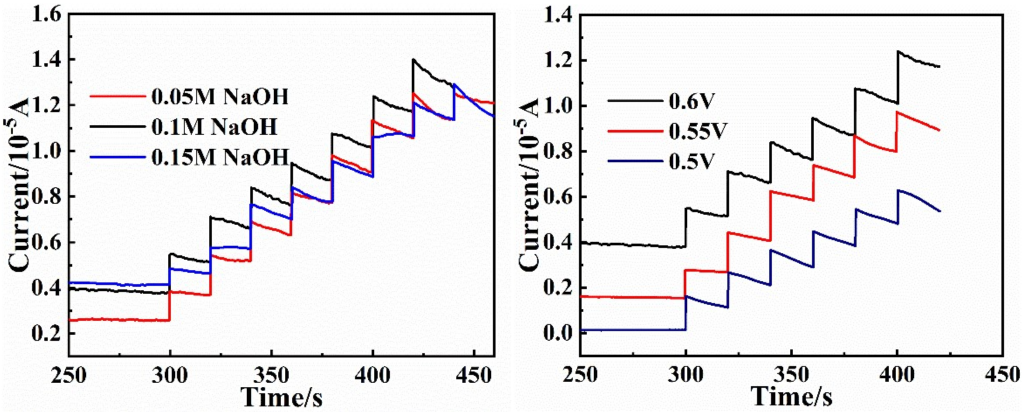


Figure S3. (a) Timing current test of $Co_3O_4$ NFs/$In_2O_3$/ITO electrodes in different concentrations of NaOH solution environment. 1 μM glucose was added every 20 s for a total of seven times. (b) Timing current test of $Co_3O_4$ NFs/$In_2O_3$/ITO electrodes at different voltages. 1 μM glucose was added every 20 s for a total of six times.

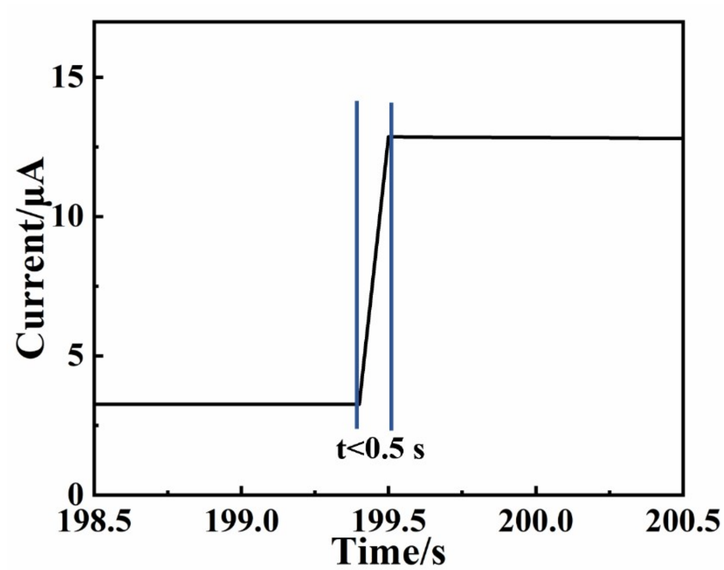


Figure S4. Current response time after addition of glucose.

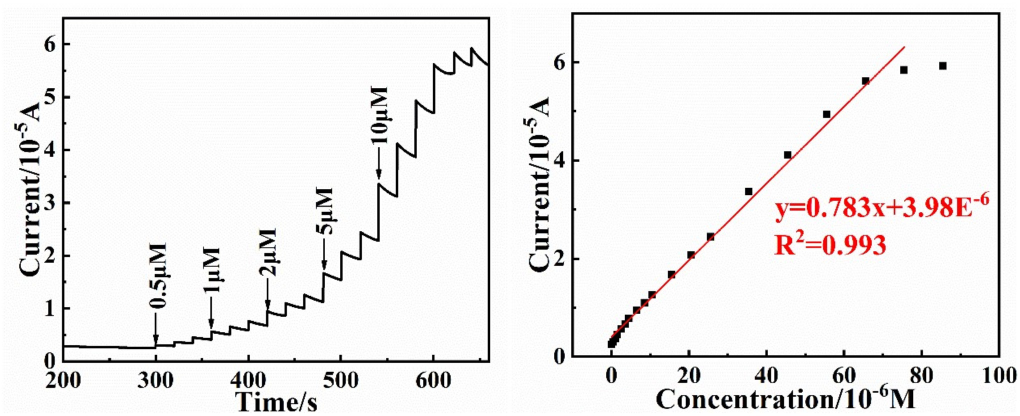


Figure S5. (a) I-t test of $Co_3O_4$ NFs at 0.6 V voltage, 0.1 M NaOH solution. (b) Calibration curve for the corresponding I-t test. The sensitivity was calculated to be 978.75 μA $mM^{-1}cm^{-2}$ and the LOD was 0.374 μM.

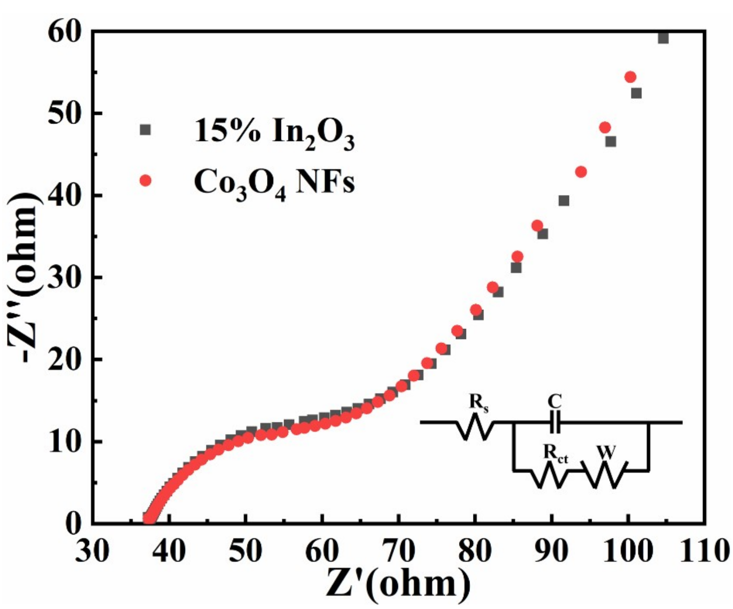

Figure S6 Impedance comparison plot of 15% $In_2O_3$ composite ratio with pure $Co_3O_4$ NFs.

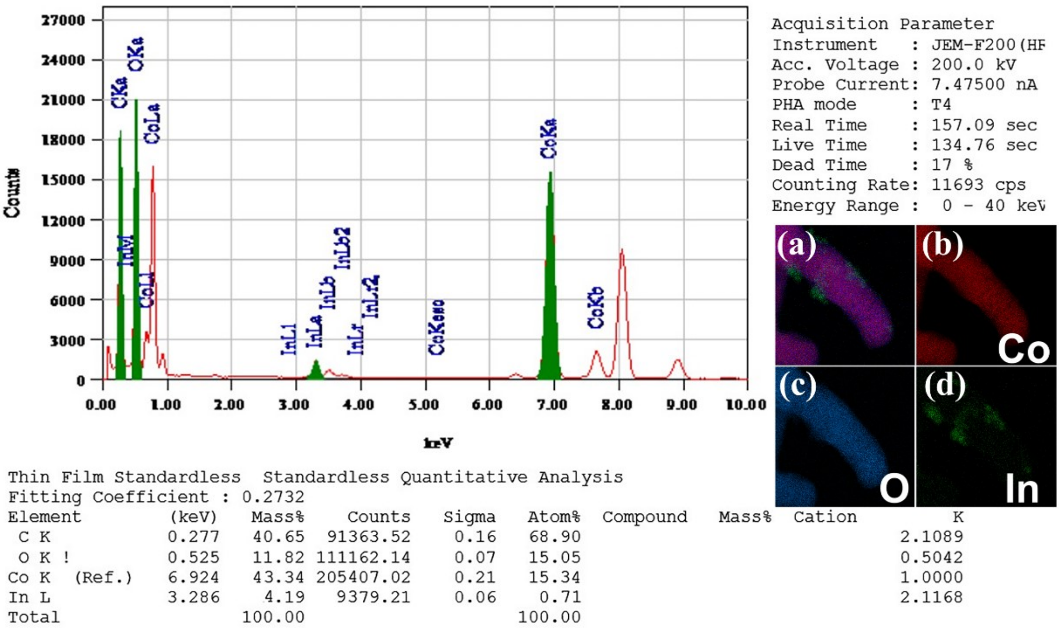


Figure S7. Point-scan EDS of $Co_3O_4$@$In_2O_3$ NFs. In light of the aforementioned images, it can be reasonably deduced that the ratio of Co3O4 to In2O3 on the surface of the material in question is approximately 23:2(wt%)

Table S1

Equivalent circuit simulations of $Co_3O_4$ NFs and $Co_3O_4$@$In_2O_3$ NFs

| Sample | $R_s(\Omega)$ | $R_{ct}(\Omega)$ |
|---|---|---|
| **$Co_3O_4$ NFs** | 37.89 | 23.53 |
| **$Co_3O_4$@$In_2O_3$ NFs** | 34.62 | 13.01 |

Table S2

Normalized comparison of current responses of various interferents and glucose in Figure 5g

| Samples | Concentration | Normalized value of response |
|---|---|---|
| Glucose | 5μM | 100% |
| UA | 0.25μM | 3.4% |
| AA | 0.25μM | 8.6% |
| L-Cysteine | 0.25μM | 1.8% |
| Sucrose | 0.25μM | 7.4% |
| Lactose | 0.25μM | 2.7% |

| | | |
|---|---|---|
| Fructose | 0.25μM | 9.2% |
| NaCl | 5μM | 3.8% |
| Glucose | 5μM | 98.8% |

Table S3

Normalized comparison of current responses of various interferents and glucose in Figure 6c

| **Samples** | **Concentration** | **Normalized value of response** |
|---|---|---|
| Glucose | 5μM | 100% |
| UA | 0.25μM | 8.5% |
| AA | 0.25μM | 7.8% |
| L-Cysteine | 0.25μM | 2.9% |
| Sucrose | 0.25μM | 5.0% |
| Lactose | 0.25μM | 7.4% |
| Fructose | 0.25μM | 7.6% |
| NaCl | 5μM | 1.4% |
| Glucose | 5μM | 99.5% |

Table S4

Comparison of current response to the addition of the same concentration of glucose in DIW and saliva (The data is sourced from Figure 5(g) and Figure 6(c)).

| **Samples** | **Concentration** | **Normalized value of response** |
|---|---|---|
| Glucose (DIW) | 5μM | 100% |
| Glucose (DIW) | 5μM | 98.8% |
| Glucose (Saliva) | 5μM | 102.1% |
| Glucose (Saliva) | 5μM | 101.4 |